

## Hybrid Controller Based Instantaneous Torque Control of Four Phase Switched Reluctance Motor

<sup>1</sup>Pushparajesh Viswanathan and <sup>2</sup>Manigandan Thathan

<sup>1</sup>Department of Electrical Engineering, Kongu Engineering College,  
Perundurai, Erode-638052, Tamil Nadu, India

<sup>2</sup>Computer Science and Engineering, P.A. College of Engineering  
and Technology, Pollachi, Tamil Nadu, Indian

---

**Abstract:** This paper proposes a new control approach for torque ripple minimization of a switched reluctance motor drive using Neural Network controller. However, it is still a very important problem to determine randomly the Neural parameters initially and then the parameters are adjusted to optimize the torque error. The approach focuses on improving the torque and flux response results in the better speed regulation and reduced torque ripple even under non liner conditions. The Intelligent controller gives high control over motor torque and speed response, reduces rise time as well as overshoot. The ANN based Direct torque control is simulated with MATLAB/SIMULINK. The simulated results shows the minimization of torque ripple for switched reluctance motor can guarantee that the settling time of speed is comparatively minimum as well as it flux and torque response is superior to traditional PWM control. The performance of the drive mainly in terms of torque ripple control is analyzed with new set of computational algorithm.

**Key words:** Four Phase Switched reluctance motor • Torque Ripple • Speed Response • Direct torque control(DTC) • Hysteresis Control • Vector Table • Instantaneous Torque

---

### INTRODUCTION

SRM drive's application has increased in the recent years because of its advantages such as simple mechanical structure, high torque/inertia ratio, adaptable to hazardous environment, high speed operation etc., Being special electrical machines family, switched reluctance motor has been used for high power and high speed application such as electric traction, rocket space launching, robotic neck movement and so on. Conventional AC/DC drives are replaced with SRM due to its advances and reliability. The primary drawback of the motor is that it has highly non-linear torque characteristics compared with other conventional motors, which causes noise and vibrations. Various torque control schemes are investigated to improve the drive efficiency in terms of minimized torque ripple and better speed response. S.K. Sahoo *et al.* in [1] specifies SRM magnetization characteristics are highly nonlinear, where torque is a complex and coupled function of the phase

currents and rotor position. An improved DTC method is proposed to 3-phase SRM, where the difference between conventional DTC and the proposed DTC to SRM has been discussed elaborately [2, 4]. A new set of space vectors is proposed for improving the torque performance of SRM [3]. The low speed and high speed operation of 6/4 SRM for control of torque is observed in [5]. A Intelligent control theory for controlling the torque production of SRM drive is discussed in [6, 14]. A short flux pattern based DTC for four phase switched reluctance drive is proposed in [7, 12]. I. Husain [8] reduce the torque ruiipple using simple current profiling technique. The disadvantage of this is the requirement of new and expensive winding topology. P. Jinupun *et al.* [9] introduce the sensoreless torque control of SRM. A NEFCLASS based Neuro Fuzzy Controller is Proposed for SRM drive to improve the torque response is discussed in [10]. Minimization of torque ripple in 8/6 SRM using fuzzy logic controller for constant dwell angles has been discussed in [11]. M. Wang *et al.* in [15] has minimized the

torque ripples by employing a Direct torque Control technique along with torque controller. The main drawback of this method is limited to low speed region. The control technique adopted by Z.Zhen *et al.* in [16] control the nonlinear characteristics of the motor by adopting a controller. The stability of this method is based on the selection of the stopping time. L.Henquires *et al.* [17] reduce the torque ripple by using hybrid controller say neuro fuzzy compensation technique. Vujicic, al and D.H. Lee *et al.* [18, 19] introduced a family of TSFs by using different secondary objectives, such as power loss minimization and drive constraint consideration. Sivaprakasam *et al.* [20] introduce novel DTC techniques to reduce the torque ripple and Mechanical vibration. Y. Sozer *et al.* [21] introduce a new method to control the excitation parameters such as turn on, turn off and the magnitude of the current. The proposed method adopts the Artificial Neural Network for selecting the voltage vectors in the DTC switching table to improve the torque and speed response of the SRM drive.

**Mathematical Model:** The most important properties of the SRMs are their nonlinear angular positioning parameters and nonlinear magnetic characteristics. Winding inductance, produced torque and Back EMF, which depends on the rotor angle causes nonlinear angular positioning parameters, while magnetic saturation is the main reason for nonlinear magnetic characteristics. The key principle which enables modeling of SRM is based on the Magnetic-position curve, which shows the linking flux versus current in different rotor angles.

The appendix contains parameters for a four phase SRM model with eight stator poles and six rotor poles, which is used in this paper. The complete mathematical model for the SRM including the magnetic and electrical equations would be achieved considering magnetic saturation.

The voltage across the motor phases is:

$$V_j = Ri_j + \frac{d\lambda_j(\theta, i_j)}{dt} + \frac{d\lambda_i}{dt} \quad (1)$$

where  $V_j$ , stands for the  $j$ th phase winding voltage,  $i_j$  for the  $j$ th phase current,  $\lambda_j$  for the linking flux,  $R$  for the ohmic resistance of the phase winding and  $\lambda_i$  for the leakage linking flux. The linking coupling between adjacent windings has been neglected.

The chain derivation formula yields

$$V_j = Ri_j + \frac{d\lambda_j(\theta, i_j)}{dt} \cdot \frac{di_j}{dt} + \frac{d\lambda_j(\theta, i_j)}{d\theta} \cdot \frac{d\theta}{dt} + \frac{d\lambda_i}{dt} \quad (2)$$

where  $\frac{d\lambda_j(\theta, i_j)}{dt}$  is the increasing inductance ( $L_{inc}$ ) and  $\frac{d\lambda_j(\theta, i_j)}{d\theta}$  is the back EMF coefficient ( $C_w$ ), both of which are dependent on current and rotor angular position.

Considering  $L_k$  as the flux leakage

$$\frac{d\lambda_i}{dt} = L_k \frac{di_j}{dt} \quad (3)$$

Replacing symbols in this equation, we have

$$V_j = Ri_j + L_{inc} \cdot \frac{di_j}{dt} + C_w \cdot \omega + L_k \cdot \frac{di_j}{dt} \quad (4)$$

The rotor mechanical kinetic equation can be listed under the function of electromagnetic torque  $T_e$  and load torque  $T_L$  based on mechanical law

$$T_e = J \cdot \frac{d^2\theta}{dt^2} + f \cdot \frac{d\theta}{dt} + T_L \quad (5)$$

$$\omega = \frac{d\theta}{dt} \quad (6)$$

$$\frac{d\omega}{dt} = \frac{1}{J} (T_e - T_L - f \cdot \omega) \quad (7)$$

where  $T_e$  electromagnetic torque,  $T_L$  Load torque,  $J$  is the moment of inertia,  $f$  is the friction ratio coefficient and  $\omega$  is angular speed.

**Direct Torque Control:** The torque production of SRM follows the reluctance principle, where the phase operates independently and in succession. Because of the serious un-linear of the magnetic circuit the general expression for the phase torque is given by

$$T(\theta, i) \approx i \frac{\partial \varphi(\theta, i)}{\partial \theta} \quad (8)$$

where  $\theta$  is the rotor position angle,  $i$  is the phase current. It is noted that in the SRM unipolar drives are normally used and thus the current in a motor phase is always

Table 1: Switching Function Table

Switching Stage of Power Converter	Terminal Voltage of Winding	Switching Function S
V1, and V2 both On	Positive Voltage	1
V1 and V2 one On and the other Off	Zero Voltage	0
V1 and V2 both Off	Negative voltage	-1

Table 3: Switching table of SRM

$T \uparrow \psi \downarrow$	$T \uparrow \psi \downarrow$	$T \downarrow \psi \uparrow$	$T \downarrow \psi \uparrow$
Vk+1	Vk-3	Vk-1	Vk+3

positive. Hence from (8), the sign of the torque is directly related to the current whereas a negative torque is produced by decreasing the stator flux amplitude with respect to the rotor position movement. The positive value and negative value are defined as “flux acceleration” and “flux deceleration. Hence, a new SRM control technique is defined as follows.

- The stator flux linkage vector of the motor is kept within amplitude hysteresis bands.
- During the stator flux vector acceleration or deceleration the torque can be controlled.

The control objective is achieved by selecting an appropriate voltage vector and also achieved by acceleration or deceleration of the stator flux vector relative to the rotor movement. It should be noted that unlike conventional DTC the torque magnitude is also a product of the instantaneous current. However a similar phenomenon to that seen in conventional DTC may be found in this control scheme. As mentioned above, the conventional ac machine DTC due to a first order delay relative to the change in stator flux. Similarly in the SR control scheme, the stator current can be found to have a first order delay relative to the change in stator flux. Thus, it can be assumed that the current is relatively constant during the control of the flux acceleration and deceleration.

Therefore unlike the conventional ac motor DTC, each phase can have three states, leading to a total of 81 possible configurations.. These voltage state vectors are defined to lie in the center of eight zones, where each zone has a width of radians. One of the eight possible states is chosen at a time in order to keep the stator flux linkage and the motor torque within hysteresis bands. The switching function table and its principle of the switching stage is defined as below.

According to the sections of instantaneous composition flux linkage, the selection of switching voltage vectors are as follows: supposed that the motor

rotates at the anticlockwise direction and the composition flux linkage of stator lies in the k th region ( $k = 1 \dots 8$ ) and the motor runs at the driving mode. If the flux linkage  $\phi$  is to increase, then the switching voltage vector should be selected as  $V_{k-1}, V_{k+1}$ . On the contrary, to decrease the flux linkage  $\phi$ , the switching voltage vector should be selected as  $V_{k-3}, V_{k+3}$ . If to increase the torque  $T$ , the switching voltage vector should be selected as  $V_{k+1}, V_{k+3}$ . On the contrary, if to decrease the torque  $T$ , the switching voltage vector should be selected as  $V_{k-1}, V_{k-3}$ . Considering the requirement of flux linkage and torque, the switching table can be depicted as Table 3, where the upward arrow means to increase and the downward arrow means to decrease.

**Control Theory of Srm**

**Conventional Dtc Method:** The Torque & Flux calculator block is used to estimate the motor flux components and the electromagnetic torque.

This calculator is based on motor equation synthesis. The  $\alpha$ - $\beta$  vector block is used to find the sector of the plane in which the flux vector lies. The plane is divided into eight different sectors spaced by 45 degrees as the sector of the plane in which the flux vector lies. The Flux & Torque Hysteresis blocks contain a two-level hysteresis comparator for flux control and torque control. The Switching table block contains two lookup tables that select a specific voltage vector in accordance with the output of the Flux & Torque Hysteresis comparators. This block also produces the initial flux in the machine. The Switching control block is used to limit the inverter commutation frequency to a maximum value specified by the user.

**Proposed DTC Control:** Due to inherent nonlinear magnetic and saliency pole nature the torque developed in SRM is well characterized by great oscillations, even in case of constant phase excitation current. In this paper, the torque ripple is minimized by selecting the suitable switching vectors using Neural compensation technique..

The block diagram of the proposed system under study is shown in Fig. 1. It consists of an SRM with its controlled Converter and power supply. Different control strategies such as Voltage control, PI and PID control and hysteresis control, can be used for the control of an SRM. However, these control techniques produce more noise and speed control is difficult. Therefore, more advanced control techniques need to be used which will minimize the drawbacks and improve the performance of the drive. Hence, controller based Direct Torque Control technique

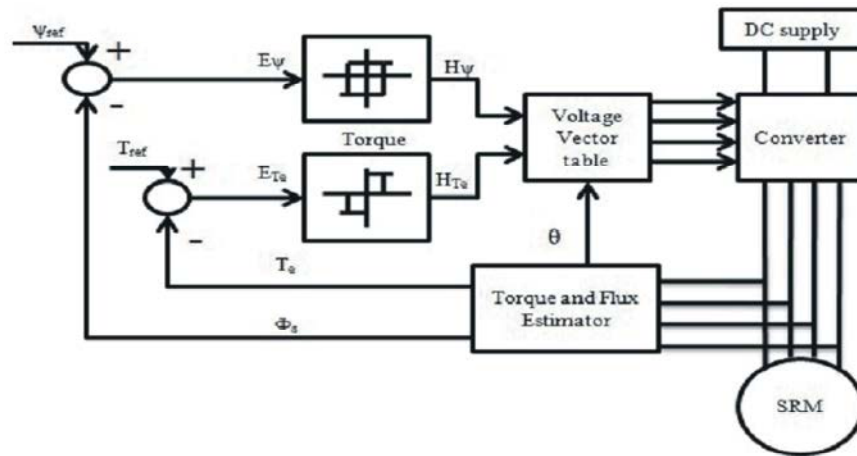


Fig. 1: Conventional DTC Block Diagram

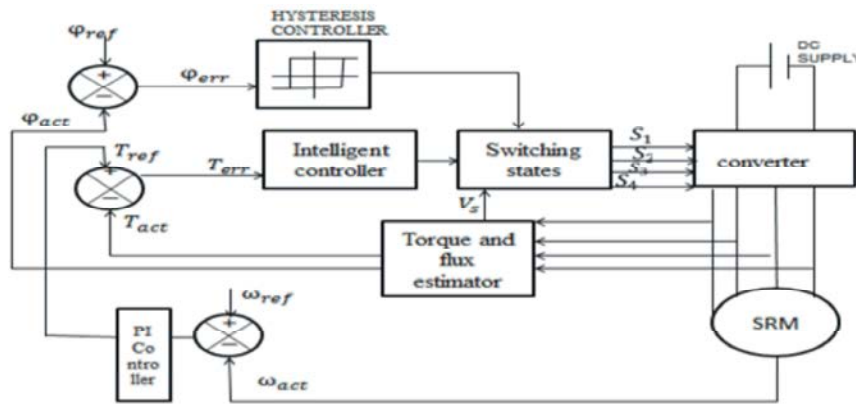


Fig. 2: Proposed Block Diagram

is studied and a Neural Network based controller is proposed. The operation of a neuro controller is to optimize the error output from a comparator which compares the reference torque and the motor actual torque. The minimized torque and the flux output along with sector is used to select the optimum voltage sector which in turn generate the firing pulses for the controlled converter. The drive is tested under constant load and at different speed conditions: First, the motor is started against its rated speed with a load torque of 2Nm. Second, the motor speed is suddenly reduced to 50% of its rated value with the above mentioned load torque followed by a removal of the disturbance after the motor reaches its steady state speed. Third the speed is further reduced to 25% of its rated speed with 2Nm load torque and the performance of the motor is analyzed.

**Modeling of Neuro Controller:** In classic DTC the stator voltage selection is made by hysteresis comparators with torque and flux magnitude errors as inputs and a

predesigned gate-pulses look- up table that selects the stator voltage vector corresponding to the desired action. This control strategy from full negative torque to full positive leads to changes that cause high torque ripple. Due to slow rotor flux dynamics, the easiest way to change the load angle is to force a change in the stator flux vector by the application of the appropriate stator voltage vector vs. The capability to actuate an torque greatly depends on the emf,  $\dot{\mu}_m$ ,  $\phi_s$ . This means that ripple frequency varies with rotor speed obtaining variable switching frequency and a wide spectrum for torque and stator current. The structure of Neural Network is shown in Figure 2. The input to the Neuro compensator is the error torque taken from comparators which compare the actual torque and the reference torque obtained from the conventional PI controller. The status Signal along with the flux signal is used to select the voltage vectors based on which the conventional asymmetric converters are operated. The Back Propagation Neuro compensator is with torque input comprising of ten linguistic rules with

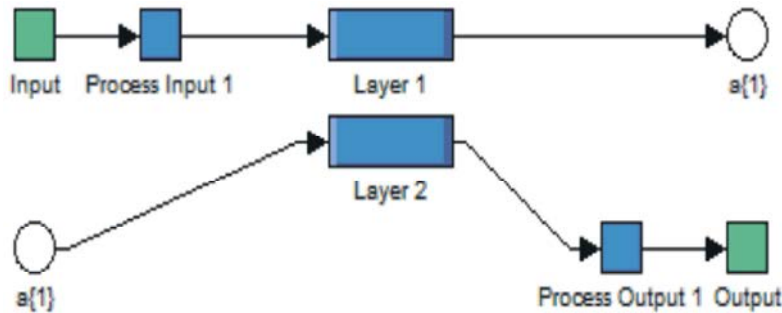


Fig. 3: Structure of Neural Network

triangular form membership functions. The Data for training in Neuro compensator is collected from simulations of SRM control and output from the compensator is varied in terms of change in speed of SRM. The rule consequents are adjusted by a Intelligent controller algorithm consist of the combination of least square minimization and back propagation which is the training procedure followed here. The dc component at each learning iteration is removed in order to avoid the ripple compensator changing the output mean value of the torque. The error minimized output from the conventional PI controller which is refereed as Reference torque is compared with the actual torque. Here, supervised learning algorithm is utilized for training the neural network. There are number of supervised learning algorithm, here back propagation feed forward algorithm is used motor torque. The torque from the comparator is fed as the input to the Neuro compensator whose output target is error free torque signal. This status signal is used to select the voltage vectors from the vector table. The Training data are obtained from simulations of steady-state simulation operation of the Switched reluctance drive system.

The DC component is removed from the motor torque at each learning iteration and only the remaining available is the ripple. This training data which is the torque ripple is tabulated against the reference torque and the angular position of the rotor. The training algorithm processes the training data to obtain the torque ripple which is interpreted as error information for each pair. The torque ripple error is reduced by readjusting the output of the Neuro compensator and the process is continued until the minimum the torque ripple limit is achieved.

First collect the input and output data by running the simulation, then using that input and output train the neural network. the samples of input and output data are as follows

INPUT	OUTPUT
707	529.4
723	543
738.6	553.2
754.3	564.9
769.6	576.4
785.5	598.4
801	600.2
816.5	611.7
832.4	623.6
848	535.3

- Step 1: Type nn tool in the command window
- Step 2: Neural network /data manager block will open. In that click new
- Step 3: Create network or data block will open where select the input and output data
- Step 4: Then click create.
- Step 5: Double click on the network name displayed in Neural network /data manager. Then new window will open in that click train menu to train the network.
- Step 6: Click export in the Neural network /data manager block. Select all and click export in the export from network /data manager block.
- Step 7: Type gensim('file name'). neural network block will open, then place the block in required location in Simulink.

**Simulation and Results:** A A 4-phase 8/6 SRM as a prototype motor is used in simulation by MATLAB/SIMULINK environment. The load torque is taken as 2 Nm and the speed of SRM is 3000 RPM. In this work, Artificial Neural Network(ANN) Controller is employed to minimize the torque ripples in switched reluctance motor. The Hysteresis Controller, conventional PI controller and Fuzzy Controller is also considered for comparison sake. The simulation is carried out for 1 seconds. For clarity over the responses, the time scale variation for flux linkages, 4 phase currents and total

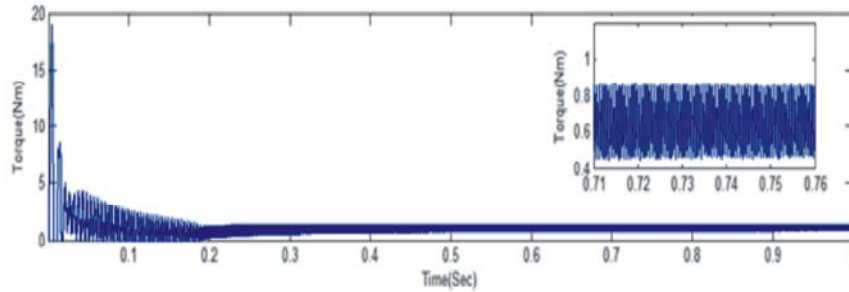


Fig. 4: Torque response for 25% of the rated torque

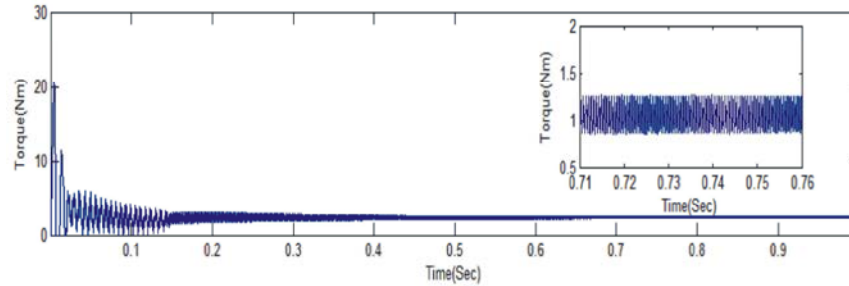


Fig. 5: Torque response for 50% of the rated torque

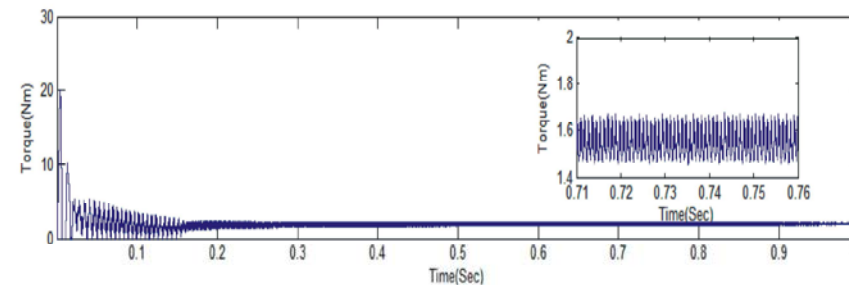


Fig. 6: Torque response for 75% of the rated torque

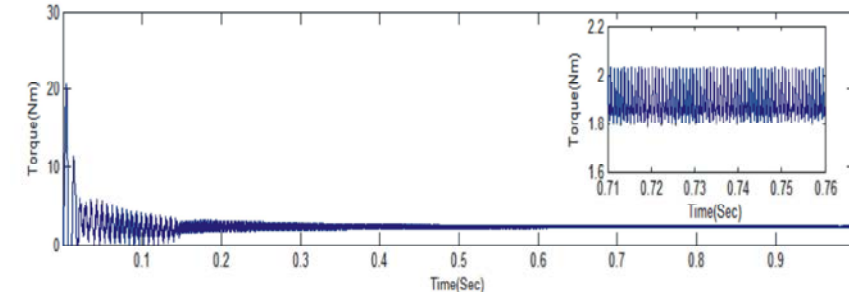


Fig. 7: Torque response for 100% of the rated torque

torque is taken as 0.71 –0.76 second and for Speed, it is taken as 0 – 1 second. Figure 4 shows the torque profile of the four phases of SRM Drives for 25% of the rated torque where the torque ripple is comparatively minimized compared to conventional controller. Figure 5 shows the torque response for 50% of the rated torque and the response in terms of speed and torque is quite superior compared to other controllers. Figure 6 depicts the torque response for 75% and Figure 7 shows the torque response

for a 100% of the rated torque. From the stimulated output the torque ripple along with speed and torque response is smoother compared to the conventional controller. It may be observed that the ANN based DTC minimize the torque ripples and also the settling time compared to the conventional controller and fuzzy controllers. Figure 8 shows the torque response under external disturbances. The band limitation of a torque transducer can be avoided by using total torque and phase torque obtained from the

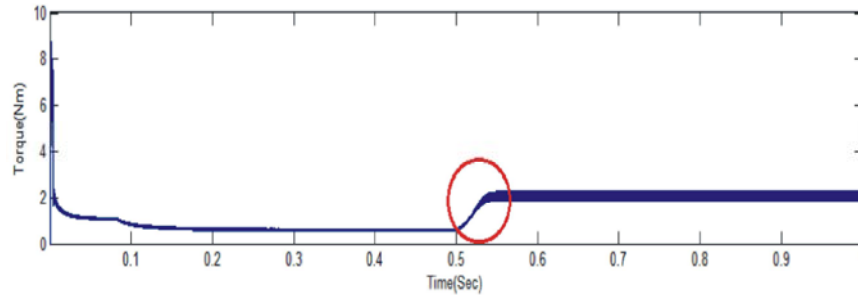


Fig. 8: Torque response under external Load disturbances

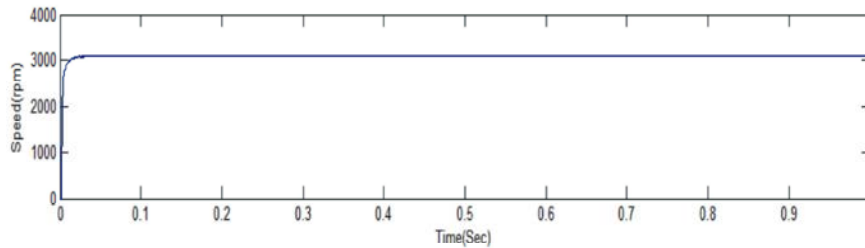


Fig. 9: Motor Speed profile for a rated speed of 3000rpm

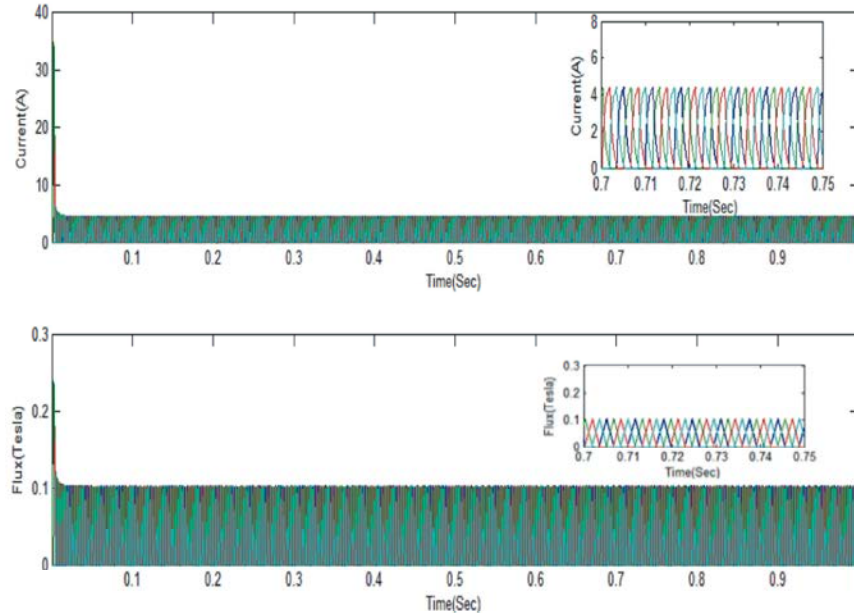


Fig. 10: Current and Flux response for 100% of the Load

torque estimator. Figure 9 shows the speed response at various load conditions which shows the settling time of speed is faster compared to the conventional controller. Figure 10 shows the current and torque profile for a load torque of 2Nm. The command speed response is very fast, typically, a few stroke angles. The torque-ripple minimization is maintained during the dynamic condition by the proposed algorithm. The tuning constants were determined and optimized using the optimization techniques through simulation. The algorithm

computation time for one cycle plays a significant role in dictating the amount of torque ripple present at an appropriate speed. The significance is even greater than the resolution of the position feedback signal. The Table 4 specifies the comparison of torque ripple in percentage for different controllers. It also shows the standard deviation of total torque ( $\sigma T$ ) and settling time ( $t_s$ ) of the responses. For the PI speed controller, which lies in outer loop, the proportional and integral gain ( $K_p$ ,  $K_i$ ) has been taken as 1.863 and 0.069 respectively.

Table 4: Comparison of Different Controller

Controller	Torque Ripple-%
Hysteresis Controller	15%
PI Controller	12%
Neuro Controller	8.55%

These parameters are obtained by means of using graphical tuning (bode plot) method which is available in control design tools of MATLAB/SIMULINK environment. These parameters are well tuned to yield better results for torque ripple reduction than without controller. Results reveal that mean torque is increased and the torque ripple coefficient and standard deviation of total torque ( $\square T$ ) are reduced for Neural Network controller.

The band limitation of a torque transducer can be avoided by using total torque and phase torque obtained from the torque estimator. Figure. 10 show the current and torque profile for a load torque of 2Nm. The command speed response is very fast, typically, a few stroke angles. The torque-ripple minimization is maintained during the dynamic condition by the proposed algorithm. The tuning constants were determined and optimized using the optimization techniques through simulation. The algorithm computation time for one cycle plays a significant role in dictating the amount of torque ripple present at a particular speed. The significance is even greater than the resolution of the position feedback signal. In Table 4, the statistical parameters such as torque ripple in Nm and torque ripple in percentage along with the settling time for various controllers are reported. It also shows the standard deviation of total torque ( $\square T$ ) and settling time ( $t_s$ ) of the responses. For the PI speed controller, which lies in outer loop, the proportional and integral gain ( $K_p$ ,  $K_i$ ) has been taken as 1.863 and 0.069 respectively.. These parameters are well tuned to yield better results for torque ripple reduction than without controller. Results reveal that mean torque is increased and the torque ripple coefficient and standard deviation of total torque ( $\square T$ ) are reduced for ANFIS controller. In FL controller, torque ripple coefficient is reduced than PI controller and Hysteresis Controller. But in ANFIS, it is still decreased when compared with PI controller and with FL controller. The settling time is also improved in both cases but ANFIS has better performance when compared with PI controller and FL. The reduced torque ripple, quick torque response with torque ripple minimized of nearly about 8% using the ANFIS based DTC compared to the conventional PI and Hysteresis controller. The

Computation period for one cycle should get completed within the encoder time period at the higher speeds of the application to obtain the best results.

In FL controller, torque ripple coefficient is reduced than PI controller and Hysteresis Controller. But in ANN, it is still decreased when compared with PI controller and with FL controller. The settling time is also improved in both cases but ANN has better performance when compared with PI controller and FL. The reduced torque ripple, quick torque response with torque ripple minimized of nearly about 7% using the Neural Network Controller based DTC compared to the conventional PI and Hysteresis controller. The Computation period for one cycle should get completed within the encoder time period at the higher speeds of the application to obtain the best results.

**Experimental Results:** In addition to the simulation results, the proposed DTC method is experimentally tested to verify the effectiveness of the proposed methods. The experimental arrangement of the proposed system is same as that of Fig. 1. A 1 kW SRM is used for this experimental verification. Fig. 17 shows the experimental arrangement of the proposed system. The input for the insulated gate bipolar transistor which is used as an inverter is fed from a four phase intelligent power module. The SPARTAN 3A / 3A DSP FPGA board is used to generate the gating pulses which are fed as the input to the inverter. The experimental results are taken with help of a Tektronix TDS 2004B digital storage oscilloscope. In addition to the simulation results, the proposed method is experimentally tested to verify the effectiveness of the proposed methods. The switching pulse pattern for a load torque of 2Nm with a rated speed of 3000 rpm is shown in Fig. 11. The voltage profile and the current profile for 100% of the load torque is shown in Fig. 12 and Fig. 13. The Current Profile for Different phases is shown in Fig 14 and 15 The experimental results for the proposed method for a load of 2Nm and a speed of 3000 rpm is shown in Fig.16. Experimental results were also taken to evaluate robustness against external load disturbances. From the experimental results, the RMS torque ripple of the proposed DTC method is more or less similar for the same method that is obtained from the simulation. The experimental setup still demands improvements in the area of digital implementation. If this is achieved the proposed DTC method is supposed to have performance similar to the results obtained in the simulation.



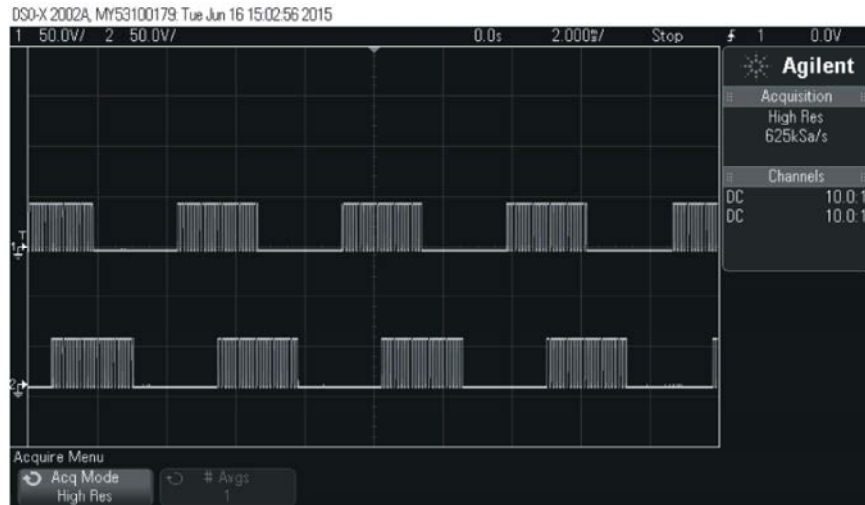


Fig. 11: Switching Pulse pattern for a load torque of 2Nm

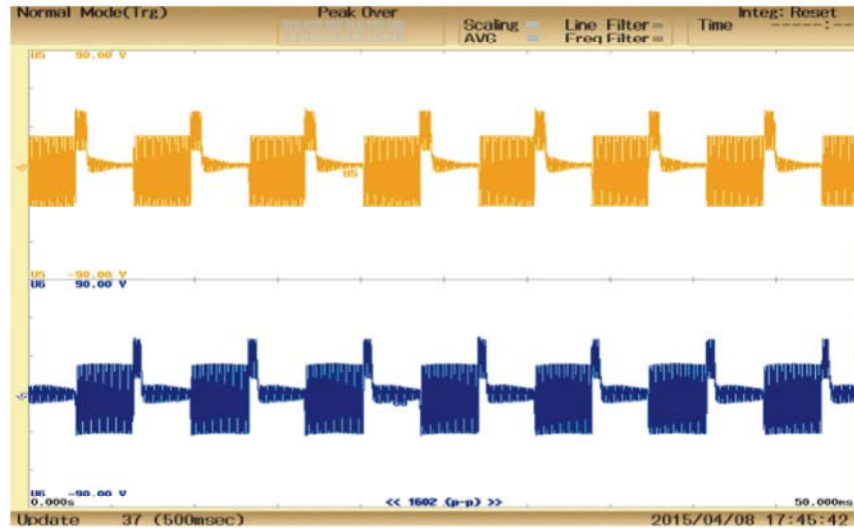


Fig. 12: Voltage Profile for Phase A and B for 2Nm load torque

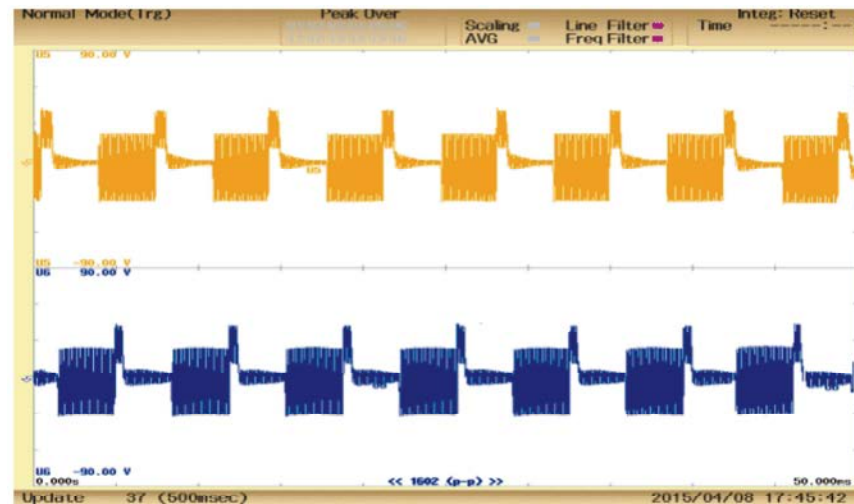


Fig. 13: Voltage Profile for Phase C and D for 2Nm load torque

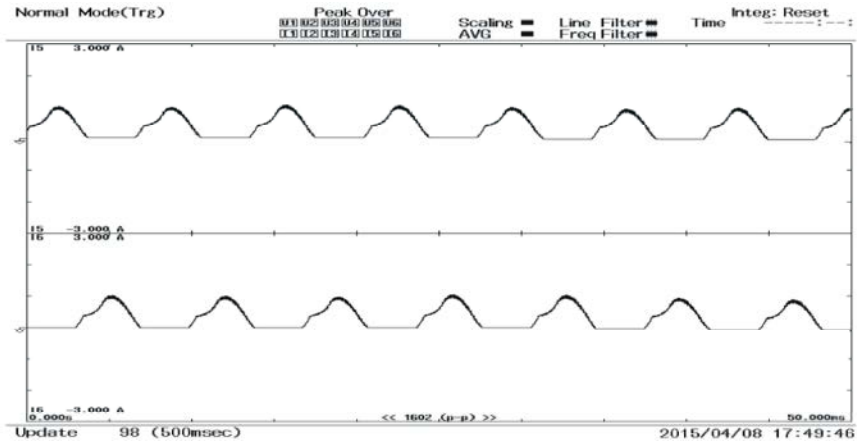


Fig. 14: Current Profile for Phase A and B for 2Nm load torque

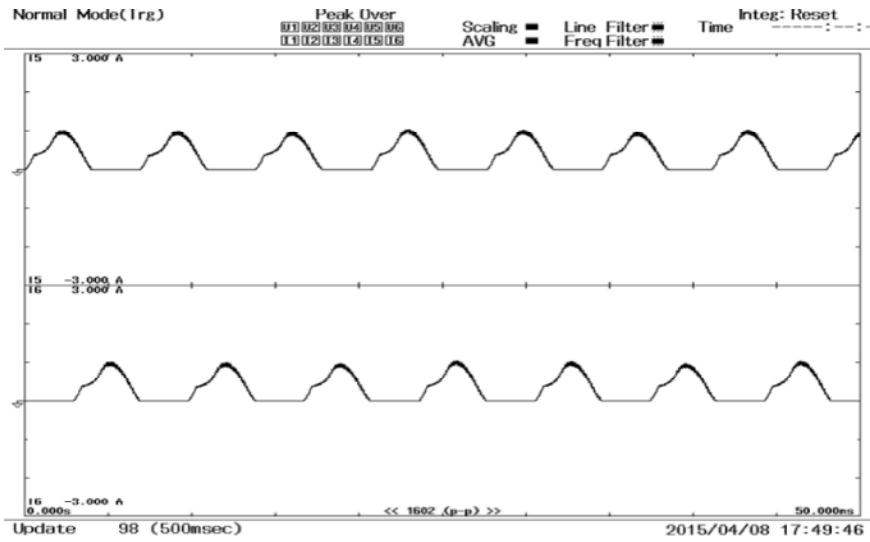


Fig. 15: Current Profile for Phase C and D for 2Nm load torque

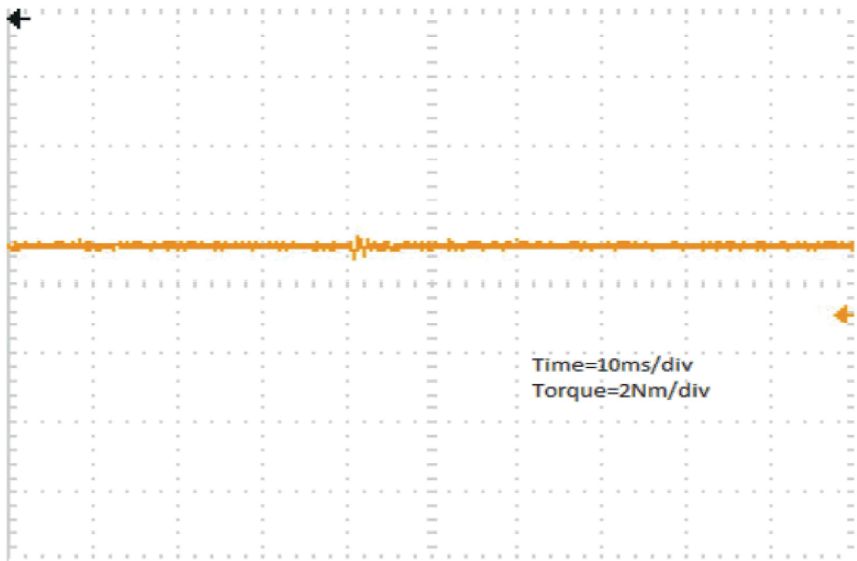


Fig. 16: Phase torque output for a load torque of 2Nm and a speed of 3000rpm



Fig. 17: Experimental Setup of 1 kW SRM with ANFIS Controller Specification of SRM

Parameter	Value
Type	8/4
No. of Phases	4
Voltage	120V
Maximum Current	18A
Stator Resistance	0.96 ohm
Unaligned Inductance	10mH
Aligned Inductance	49mH
Inertia	0.008 Kg.m <sup>2</sup>
Friction	0.01 N.m.s
Max.Flux Linkage	0.3 V.s

### CONCLUSION

The performance of the proposed optimization technique is comparatively evaluated with conventional techniques and existing literatures. Simulation results prove that the proposed Neural Network algorithm is able to reduce the torque ripple at different operating conditions compared to convention methods. The settling time of the torque and the response time of the speed can be reduced in the proposed technique compared to the conventional method which in turn increases the efficiency of the machine. The relatively recent approaches of torque-ripple minimization attempt smooth torque over a wide speed range. Although the torque ripple will progressively increase with speed, these new approaches are highly desirable for applications where the speed range varies widely. The SRM with its extended constant-power region of operation can be utilized in such applications to reduce the cost of gearing.

### REFERENCES

1. Sahoo, S.K., S. Dasgupta, S.K. Panda and J.X. Xu, 2012. A lyapunov function based robust direct torque controller for switched reluctance motor drive system, *IEEE Trans.Power Electron.*, 27(2): 555-564.
2. Xue, X.D. and K.W.E. Cheng, 2009. Optimization and Evaluation of Torque Sharing Functions for Torque Ripple Minimisation in Switched Reluctance Motor: *IEEE Transaction on Power Electronics*, 24(9).
3. Cheok, A. and Y. Fukuda, 2002. A new torque and flux control method for switched reluctance motor drives. *IEEE Transactions on Power Electronics*, 17(4): 543-557.
4. H. Guo. Considerations of direct torque control for Switched reluctance motors. in: *Proceedings of the 2006 IEEE International Symposium on Industrial Electronics, ISIE, 2006, 2321-2325.*

5. Cheok, A. and P. Hoon, 2000. A new torque control method for Switched reluctance motor drives. in 26<sup>th</sup> Annual conference of the IEEE Industrial Electronics Society, IECON, pp: 387-392.
6. Silverio Bolognani and Mauro Zigliotto, Fuzzy Logic Control of a Switched Reluctance Motor Drive, IEEE Transactions on Industry Applications, Vol. 32, No. 5, September / October 1996, pp: 1063-1068.
7. Jeong, B., K. Lee, *et al.*, 2005. Direct torque control for the 4-Phase switched reluctance motor drives in Proceedings of the 2005 IEEE International Conference on Electrical Machines and Systems, ICEMS 2005, 2005, 524-528.
8. Husain, I., 2002. Minimization of torque ripple in srm drives. IEEE Transactions on Industrial Electronics, 49(1): 28-39.
9. Jinupun, P., 1998. P.Luk. irect torque control for sensorless switched reluctance motor drives. in: Proceedings of the 7<sup>th</sup> International Conference on Power Electronics & Variable Speed Drives, pp: 329-334.
10. Ali Akcayola, M. and Cetin Elmas, 2005. NEFCLASS-based neuro fuzzy controller for SRM drive, Journal of Engineering Applications of Artificial Intelligence 18: 595-602.
11. Srinivas, P. and P. Prasad, 2010. Torque ripple minimization of 8/6 switched reluctance motor with fuzzy logic controller for constant dwell angles in Proceedings of the IEEE International Conference on Power Electronics Drives and Energy Systems, 2010.
12. Song, G., Z. Li, *et al.*, 2008. Direct torque control of switched reluctance motors in Proceedings of the 2008 IEEE International Conference on Electrical Machines and Systems, ICEMS, pp: 3389-3392.
13. Miller, T., 1993. Switched Reluctance Motors and their Control. Magna Physics & Oxford.
14. Staton, D., W. Soong and T. Miller, 1995. Unified theory of torque production in switched reluctance and synchronous reluctance motors. IEEE Transactions on Industry Applications, 31: 329-337.
15. Wang, M., 2011. Four phase switched reluctance motor direct torque control in Proceedings of the 2011 IEEE international Conference on Measuring Technology and Mechatronics Automation, pp: 251-254.
16. Zhen, Z., W. Terry and C. Juan, 2000. Modeling and nonlinear control of a switched reluctance motor to minimize torque ripple in Proceedings of the 2000 IEEE International Conference on Systems, Man and Cybernetics, 5: 3471-3448.
17. Henriques, L., L. Rolim, *et al.*, 2000. Torque ripple minimization of switched reluctance drive using a neuro-fuzzy compensation. IEEE Transactions on Magnetics, 36(5): 3592-3594.
18. Lee, D.H., J. Liang, Z.G. Lee and J.W. Ahn, 2009. A simple nonlinear logical torque sharing function for low torque ripple SR drives, IEEE Trans. Ind. Electron., 56(8) 3021-3028.
19. Vujicic, V.P., 2012. Minimization of torque ripple and copper losses in switched reluctance drive, IEEE Trans. Power Electronics, 27(1): 388-399.
20. Sivaprakasam, A. and T. Manigandan, 2015. An alternative scheme to reduce torque ripple and mechanical vibration in direct torque controlled permanent magnet synchronous motor', Journal of Vibration and Control, 21(5): 855-871.
21. Sozer, Y. and D.A. Torrey, 2007. Optimal turn-off angle control in the face of automatic turn-on angle control for switched-reluctance motors, IET Electr. Power Appl., 1(3): 395-401.